IEEE Access
Multidisciplinary ⋮ Rapid Review ⋮ Open Access Journal

Received 4 September 2022, accepted 27 September 2022, date of publication 3 November 2022, date of current version 8 November 2022.

Digital Object Identifier 10.1109/ACCESS.2022.3218342

RESEARCH ARTICLE

Flexible Patch Antenna Array Operating at Microwaves Based on Thin Composite Material

HUSAMELDIN ABDELRAHMAN ELMOBARAK[1], MOHAMED HIMDI[2], XAVIER CASTEL[2], SHARUL KAMAL ABDUL RAHIM[3], AND TAN KIM GEOK[4]

[1]Faculty of Engineering Science, Omdurman Islamic University (OIU), Omdurman 14415, Sudan
[2]Univ Rennes, CNRS, IETR-UMR 6164, F-35000 Rennes, France
[3]Wireless Communication Center (WCC), Universiti Teknologi Malaysia (UTM), Skudai 81300, Malaysia
[4]Faculty of Engineering and Technology, Multimedia University, Melaka 75450, Malaysia

Corresponding author: Husameldin Abdelrahman Elmobarak (husam.a@oiu.edu.sd)

This work was supported in part by the European Union through the European Regional Development Fund, in part by the Ministry of Higher Education and Research, in part by the Région Bretagne, in part by the Département des Côtes d'Armor and Saint-Brieuc Armor Agglomération through the CPER Projects 2015-2020 MATECOM and SOPHIE/STIC and Ondes and in part by the Telekom Malaysia Berhad under Grant MMUE/220012.

ABSTRACT This paper presents an innovative route to fabricate conformal patch antenna arrays based on a flexible mesh-style conductive fabric / E-glass fiber composite laminate with improved performance at microwaves. On the one hand, the ohmic loss in the antenna array is restricted by integrating a highly conductive fabric into an E-glass fiber composite laminate and by using it as feeding lines and radiating elements after its precise machining by laser technology. On the other hand, the dielectric loss is restricted by inserting a foam layer (with dielectric characteristics close to those of the air) between the laminate substrate and the ground plane which is made of the highly conductive mesh-style fabric. The bending effect of the antenna array on its radiation pattern is minimized by applying a phase offset through phase shifters at the feeding lines of the most curved patches. The high radiation performance in gain and efficiency at 5.8 GHz (11.9 dBi and 75% in a flat configuration, and 8.7 dBi and 75% in a 50 mm-radius bending configuration, respectively), the seamless integration process, and the flexible mechanical properties of such composite antenna arrays pave the way for their promising and efficient integration into various devices, objects, and vehicles made of composite laminate materials.

INDEX TERMS Composite antenna, flexible antenna, conformal antenna array, conductive fabric, 5G.

I. INTRODUCTION

Nowadays, people depend on composite materials in numerous aspects of their lives. The composite material is defined as a combination of two or more different materials, namely reinforcement, fillers, and binders. After combination, the resulting material exhibits enhanced properties as compared to those of the individual materials. Conventional man-made composite materials are classified into three main groups: Polymer Matrix Composites (PMC), Metal Matrix Composites (MMC), and Ceramic Matrix Composites (CMC) [1]. The most widely used is the PMC group, also known as Fiber Reinforced Polymers (FRP). This type of composite material is constructed from a resin, as the matrix, and a variety of reinforcement fibers such as aramid, carbon, or glass. The PMC materials possess abundant outstanding features that can be utilized in a variety of applications [2].

In the aerospace industrial field, approximately 50% of the constituent materials of the aerospace vehicles, such as military fighter aircrafts, helicopters, satellites, civil transport aircrafts, launch vehicles, and missiles, are made of PMC [1], [3], [4], [5]. The primary benefits of the PMC materials are assembly simplification, lightweight, and mechanical strength. Wireless communication applications are also essential to aerospace vehicles. Therefore, integrating the antennas into the vehicle's body through their fabrication from the same materials enable them to be embedded and conformed [6], [7].

In the automotive field, PMC materials offer high mechanical strength, lightweight, safer, and accordingly more

The associate editor coordinating the review of this manuscript and approving it for publication was Wanchen Yang.

efficient fuel consumption [8], [9], [10]. Nowadays, the vehicle to vehicle (V2V) communication applications are growing rapidly seeking safer driving and comfortable transportation [9], [11]. Consequently, the integration of antennas into the vehicle's body will simplify the design of V2V systems.

PMC materials based on carbon fiber or glass-fiber reinforcements and thermosetting or thermoplastic resins are used to fabricate most parts of electronic device covers such as laptops, tablets, and mobile phones. Embedded antennas into such covers will be of great interest [12], [13]. From the application point of view, the wide range of PMC applications in our current and future daily life implies that this major family of materials will play a very important role in future wireless technology applications. Therefore, the question arises if efficient antennas and radiofrequency (RF) components can be fabricated from PMC materials to simplify their manufacturing and enable them to communicate effectively.

To fabricate an antenna from PMC material, this needs to be used, (i) as a dielectric substrate and (ii) as a conductive material for the radiating elements, the feeding lines, and the ground planes. The conductive material has to be embedded in both PMC surfaces for an integrated and compact structure. A highly conductive material is essential to ensure low ohmic loss and high efficiency at microwaves. Nevertheless, the selection of the conductive material must not only base on its conductivity values but also on its ability to be integrated into the PMC material.

Metals are commonly used as radiating elements, feeding lines, and grounds planes for antennas and RF components because of their high conductivity. However, the nature of the metal, its cost, its weight, and its chemical affinity with resins to keep the structural strength can limit its use and make it unsuitable for integration in PMC materials. Recent studies have presented various conductive materials as a replacement for metals to design full composite antennas [14], [15], [16], [17]. Advanced Carbon-Fiber Composite (CFC) materials are widely used in a variety of applications as a suitable replacement for conventional conductors (metals) because of their low weight, high strength, and easiness to be integrated for PMC fabrication [18], [19], [20], [21]. Two types of CFCs are highly conductive, namely the Carbon Nanotube Composites (CNT) [22], [23] and the Reinforced Continuous Carbon Fiber (RCCF) [24]. The individual conductive CNTs possess outstanding mechanical and electrical properties. However, issues such as high contact resistances between nanotubes and inhomogeneous dispersion of the nanotubes affect the transfer of individual properties to those of the composite laminate [25], [26]. The RCCF is most commonly fabricated from carbon fibers oriented in a specific direction(s), *i.e.* a fabric embedded into thermosetting resin. Its electrical conductance depends on the thickness and the weave of the fabric, the number of carbon filaments per fiber, the diameter, and the intrinsic conductivity of the carbon filaments [27], [28], [29]. However, the study presented in [30] shows that conductive carbon fabric used as an antenna radiating element at operating frequencies higher than 3 GHz is not relevant due to the ohmic loss at high frequencies. Both materials (CNT and RCCF) exhibit weak conductivity values (Table 1) compared with that of a metal reference such as copper (5.9×10^7 S/m) [14], [30]. Consequently, the low conductivity leads to the weak performance of the antennas made of such materials, especially for applications requiring high gain and high efficiency such as antenna array. Moreover, most of these materials are either not suitable for integration with PMC or require further long and complicated processes to be synthesized, such as CNT materials, making the antenna fabrication process more complex as well. A transparent and highly conductive mesh-style fabric integrated into a polymer layer to fabricate a transparent Ultra-Wideband antenna (UWB) has been presented in [31]. This conductive material exhibits attractive properties such as high conductivity, high flexibility, and a mesh-style fabric which makes it suitable to be integrated as conductive layers in PMC materials.

Conformal antenna arrays are required in many applications of PMC materials especially when the arrays should be fixed on curved surfaces of vehicles, or near the edges of composite objects and devices. Hence the present study investigates the microwave performance of flexible PMC (FPMC) antenna arrays based on a highly conductive mesh-style fabric integrated on the surface of a thin E-glass fiber / epoxy resin composite laminate for conformal applications. The conductive fabric is used to fabricate the radiating elements, the feeding lines, and the ground planes of the antenna arrays with the patterns of elements machined precisely by laser technology.

TABLE 1. Comparison of the performance of the composite antennas made of various conducting materials.

[Ref.]	Material	Conductivity (S/m)	Operating frequency (GHz)	Maximum gain (dBi)	Efficiency (%)
[24]	CFC	8×10^3	1.5-3	0.2	38
[32]	RCCF	3.5×10^3	1.7-3	-2.0	39.9
[33]	SWCNT	3×10^4	0.9-5.7	3.5	Not available
[28]	MWCNT	4×10^3	3.1-10.6	2.1	45
[14]	Conductive carbon fiber tissue	18×10^3	1-4.6	3.0	65
[34, 35]	Shieldit Super	1.1×10^5	3.3-10.5	6.8	67
[31]	Conductive mesh fabric	2×10^5	3-13	3.1	80

Thus, the paper is organized as follows. First, the fabrication of a single-side conductive FPMC panel is presented in Section II. Based on the design of an FPMC single patch antenna described in Section III, the design and fabrication processes of an antenna array are presented in Section IV. The bending effect on the FPMC antenna array is detailed and discussed in Section V. Finally, conclusions are drawn in Section VI.

II. SINGLE SIDE CONDUCTIVE FPMC LAMINATE FABRICATION

Prior to the fabrication of the conductive FPMC laminate, the characteristics of the composite materials, namely the conductive and dielectric properties, are first presented.

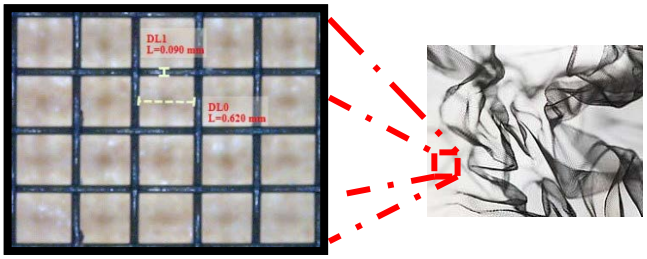

(a) (b)

FIGURE 1. Conductive mesh-style fabric. (a) Zoom (×50). (b) Photograph.

A. HIGHLY CONDUCTIVE MESH-STYLE FABRIC

A highly conductive mesh-style fabric (supplied by Less EMF Inc, USA) is utilized as the conductive layer of the single composite antenna and antenna arrays. The fabric is consisting of woven mesh polyester fibers coated with nickel/zinc blackened copper for better corrosion resistance. It exhibits ultra-lightweight (15 g/m^2) and high mechanical flexibility. The fabric mesh is characterized by a pitch of 620 μm, a strip width of 90 μm (see Fig. 1(a) and (b)) and a thickness $d = 57$ μm. The sheet resistance R_s measured by a standard four-probe setup is equal to 0.09 Ω/sq. The effective electrical conductivity σ_{eff} is computed from (1) [14], as follows:

$$\sigma_{eff} = \frac{1}{R_s \times d} \tag{1}$$

leading to a value $\sigma_{eff} = 0.2 \times 10^6$ S/m.

B. FABRICATION OF THE CONDUCTIVE FPMC LAMINATE

The one-sided conductive composite laminate was fabricated by the infusion process. One ply of the conductive fabric (15 g/m^2) and one ply of an E-glass fiber mat fabric (30 g/m^2) were stacked onto a glass slab, one above the other. Placed under vacuum (−0.8 bar) with a plastic bag as shown in Fig. 2, the conductive and mat fabrics were infused jointly with a liquid epoxy resin (with 19% by weight of hardener). It was left for 4 hours at room temperature to complete the polymerization reaction. The thin conductive FPMC laminate (0.3 mm-thick, Fig. 3) was then suitable for release without any post-bake. The FPMC laminate is therefore composed of the conductive mesh-style fabric located on its front side (conductive part of the laminate) and of the E-glass fiber mat fabric on its back side (dielectric part of the laminate).

C. FPMC DIELECTRIC CHARACTERISTICS

In order to measure the dielectric characteristics of the FPMC material, a pure E-glass fiber composite laminate has been fabricated following the same steps as described in Section II.B without any conductive fabric.

The dielectric properties were measured using an open-ended coaxial probe coupled to a vector network analyzer. The relative permittivity (ε_r) is equal to 2.7 and the loss tangent ($tan\delta$) is equal to 0.02 at 6 GHz.

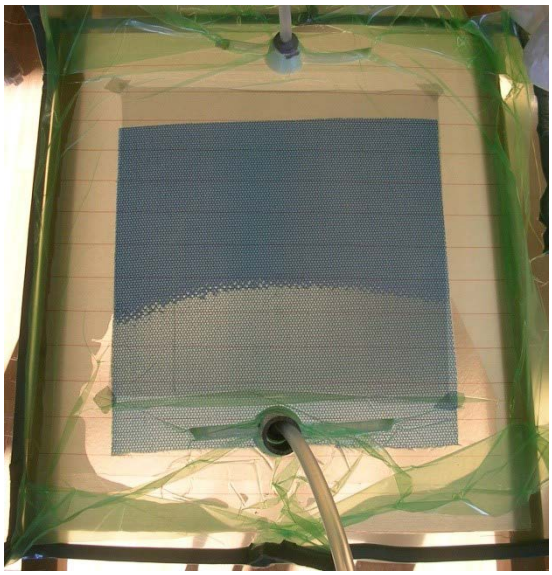

FIGURE 2. Conductive FPMC laminate during its fabrication by the infusion process. Note the resin front in the conductive mesh-style fabric and E-glass fiber mat.

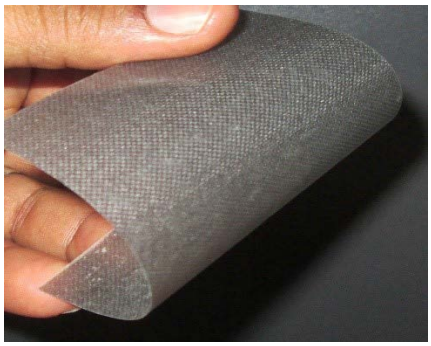

FIGURE 3. 0.3 mm-thick conductive FPMC laminate after its fabrication.

III. FPMC SINGLE PATCH ANTENNA DESIGN

Before the design and fabrication of the antenna arrays based on the flexible PMC material, a single patch antenna was designed to operate at the resonance frequency $f_r = 5.8$ GHz. The geometry of the patch antenna is inspired by [36], where L_p is the length of the radiating patch and W_p is the width of the radiating patch. The feeding line (W_{f2} width) is designed to match a 50 Ω input impedance at 5.8 GHz. The extra strip (W_{f1} width) between the feeding line and the patch is a quarter-wavelength transmission line to improve the matching. The dimensions of the patch antenna are detailed in Table 2, according to its layout depicted in Fig. 4(a).

TABLE 2. Dimensions of the single FPMC patch antenna.

Parameters	Patch antenna without the foam layer (mm)	Patch antenna with the foam layer (mm)
W	50.0	50.0
W_p	17.6	17.6
W_{f1}	0.6	0.8
W_{f2}	1.0	5.5
L	55.0	60.0
L_p	14.2	20.5

The conductive FPMC was designed with a thickness of $d_1 = 0.3$ mm to keep the optimum flexible mechanical properties of the laminate. It is well known that a microstrip patch antenna presents low efficiency and bandwidth [35]. Moreover, the conductive fabric exhibits a lower conductivity than that of a usual metal sheet such as copper. Therefore, the ohmic loss has to be considered. Based on the numerical results, the antenna exhibits a bandwidth of 89 MHz at -10 dB and a gain of about 1.9 dBi at the 5.8 GHz center frequency, as shown in Figs. 5 and 6(a) respectively. The antenna efficiency equals 45%. Furthermore, the low efficiency and performance of the designed microstrip antenna are also due to the thinness of the substrate (0.3 mm-thick) which induces narrow strips of the transmission line, and thereby increases the loss in the feeding line. The electric field between the antenna (including the feeding line) and the ground plane being strongly confined into the thin dielectric substrate (with $tan\delta = 0.02$), this contributes also to the weak antenna performance.

To overcome this result, an air gap layer has been inserted between the FPMC material and the ground plane (Fig. 7) to decrease the dielectric loss and thus improve the bandwidth and efficiency [37].

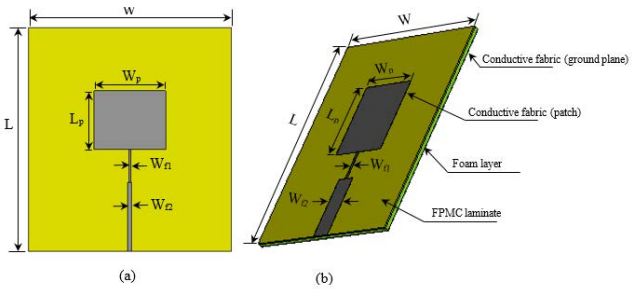

FIGURE 4. Layout and dimensions of the single FPMC patch antenna. (a) without the foam layer. (b) with the foam layer.

The air gap layer decreases the effective permittivity ε_{eff} and hence, strengthens the fringing field at the patch periphery and increases the radiated power [38], [40], [41]. So the relative permittivity of the FPMC layer ε_r has to be replaced with ε_{eff} of the multilayered structure as shown in Figs. 4(b) and 7, and calculated from (2) according to [42], where d_1 is the FPMC layer thickness and d_2 is the air gap layer thickness.

$$\varepsilon_{eff} = \frac{\varepsilon_r(d_1+d_2)}{(d_1+\varepsilon_r d_2)} \tag{2}$$

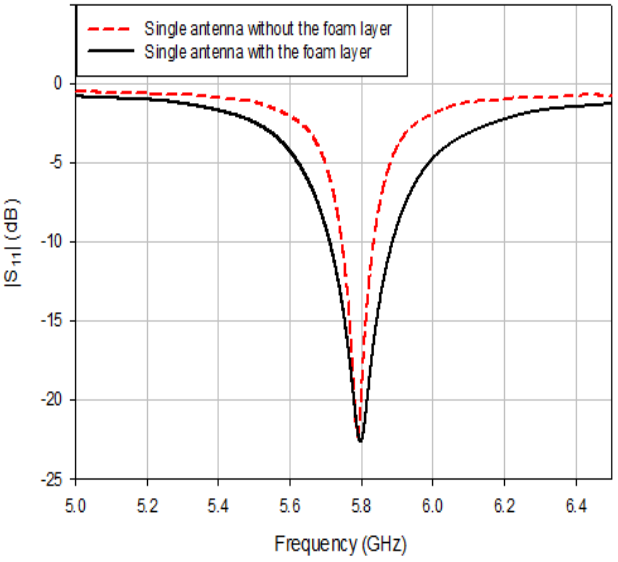

FIGURE 5. Simulated reflection coefficient magnitudes of the single FPMC patch antenna, with and without the foam layer.

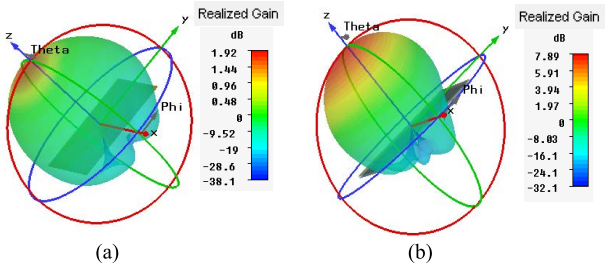

FIGURE 6. Simulated radiation patterns and realized gains of the single FPMC patch antenna at 5.8 GHz. (a) without the foam layer. (b) with the foam layer.

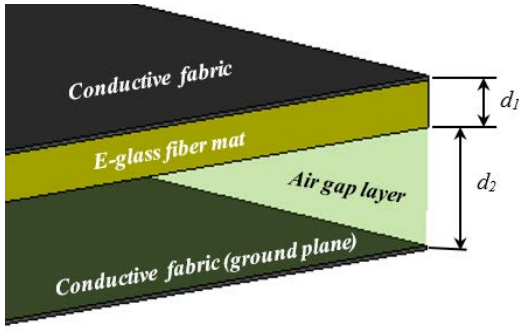

FIGURE 7. Air gap layer inserted between the conductive FPMC laminate and a conductive fabric (ground plane).

On the one hand, to maintain a constant air gap thickness between the FPMC layer and a conductive fabric used as a ground plane, this should be suspended away at the required distance d_2, which is practically not possible. Thus, a thin layer of foam with a thickness of d_2 has been used here (Rohacell foam with dielectric characteristics very close to those of air: $\varepsilon_r = 1.05$ and loss tangent $tan\delta = 0.0003$ at 10 GHz).

On the other hand, the foam layer is set to 1 mm to keep the flexible properties of the microstrip antenna. Nevertheless, the additional foam layer affects the matching of the transmission lines and accordingly, the microstrip feeding and quarter-wavelength transmission lines widths have been adjusted to keep the perfect impedance matching. The new values of W_{f1} and W_{f2} are given in Table 2 associated with $\varepsilon_{eff} = 1.17$, $d_1 = 0.3$ mm, and $d_2 = 1$ mm. The numerical results of such a single FPMC patch antenna with an additional foam layer exhibit a strong improvement of the gain (7.9 dBi) and the efficiency (71%) at 5.8 GHz (Fig. 6(b)) against 1.9 dBi and 45% without the foam layer.

IV. FPMC ANTENNA ARRAY DESIGN AND FABRICATION

Based on the numerical results of the single patch antenna, the FPMC antenna array has been designed and fabricated. The array consists of 4 × 1 rectangular patches and each patch is excited through a quarter-wave transformer impedance matching feeding line. Patches are spaced at $\lambda_r/2$ working wavelength between the centers of two adjacent ones (Fig. 8).

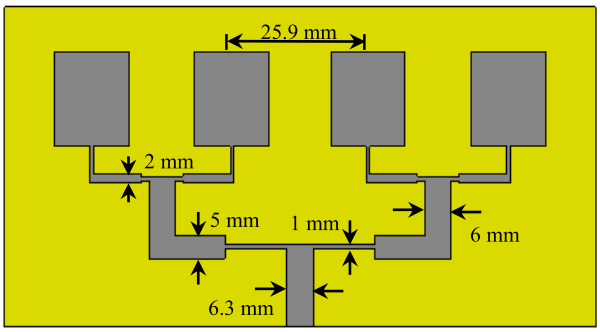

FIGURE 8. Layout and dimensions of the FPMC antenna array.

To fabricate the FPMC antenna array, the same process described in Section II.B was used. The antenna array pattern was subsequently formed through the laser etching (LPKF ProtoLaser S124102) of the embedded top-layer mesh-style fabric. The infrared laser beam ($\lambda = 1080$ nm) was focused accurately on the conductive fabric (25 μm × 25 μm laser spot size) with the appropriate settings, such as laser scan speed (400 mm/s), and power fluency (10 W/spot). Using these parameters, the laser beam ablated only the upper conductive fabric of the FPMC laminate without damaging the dielectric bottom layer. Then the 1 mm-thick foam layer was sandwiched between the single-side conductive FPMC laminate and a conductive fabric layer (ground plane) as shown in Fig. 9. To fix the SMA connector onto the microstrip feeding line of the antenna array, the surface of the FPMC was locally scratched gently to peel off the resin layer and to release the conductive fabric. Afterward, the SMA connector was fixed using a conductive silver epoxy glue to ensure reliable electrical interconnection (the conductive fabric was not suitable for conventional soldering). The return loss and radiation patterns were measured and compared with those of the simulated ones in a flat configuration. The results fit well as shown in Figs. 10 and 11. The measured gain at 5.8 GHz (11.9 dBi) is in good agreement with the simulated one (12.9 dBi), such as the efficiencies: 75% against 76%, respectively (Table 3).

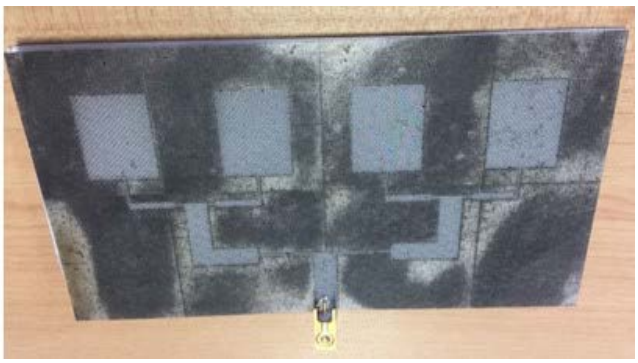

FIGURE 9. Photograph of the FPMC antenna array. The laser-etched areas are in dark color and the pristine areas which define the antenna array pattern are in a bright color.

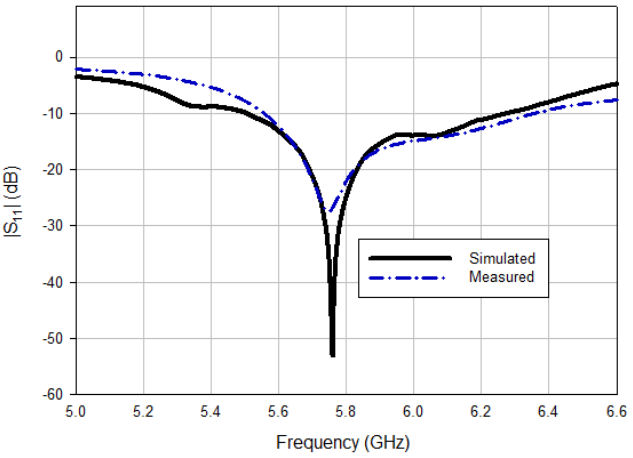

FIGURE 10. Simulated and measured reflection coefficient magnitudes of the FPMC antenna array in the flat configuration.

V. BENDING EFFECT ON THE FPMC ANTENNA ARRAY

In order to evaluate the behavior of the FPMC antenna array in conformal situations, an assessment of the antenna radiation performance was carried out at 5.8 GHz. To simulate the bending effect, the FPMC antenna array was first curved on air cylinders (Fig. 12) with various bend radii (50 mm, 75 mm, and 100 mm).

The simulated results depicted a deformation of the radiation patterns as the cylinder radius decreases up to 50 mm (Fig. 13). By using an air cylinder with a radius of 100 mm, the radiation pattern remains satisfactory with a noticeable decrease in the main lob level. However, the side lobs level (SLL) increases strongly when the radius is lowered from 75 mm to 50 mm.

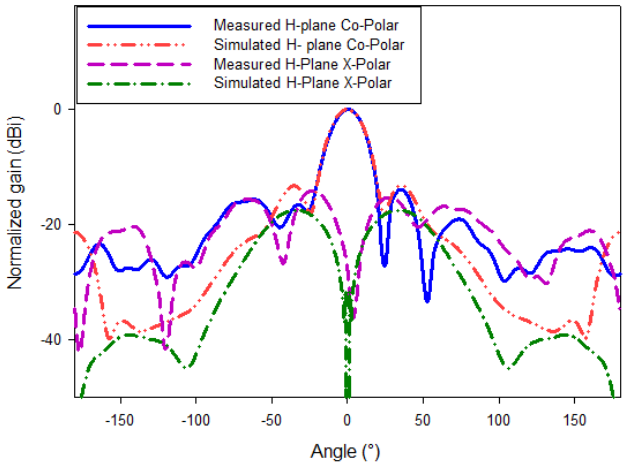

FIGURE 11. Simulated and measured radiation patterns of the FPMC antenna array at 5.8 GHz in the flat configuration.

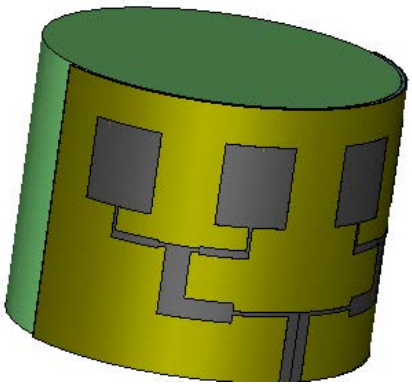

FIGURE 12. Simulated FPMC antenna array curved on an air cylinder.

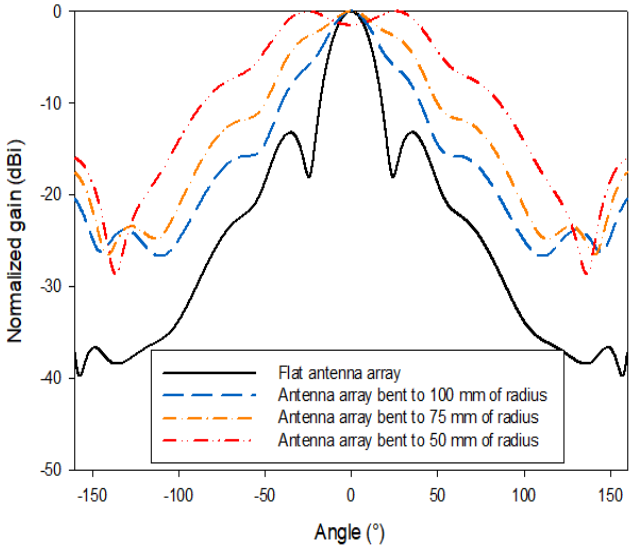

FIGURE 13. Simulated *H*-plane co-polar radiation patterns of the FPMC antenna array in flat and various bending configurations at 5.8 GHz.

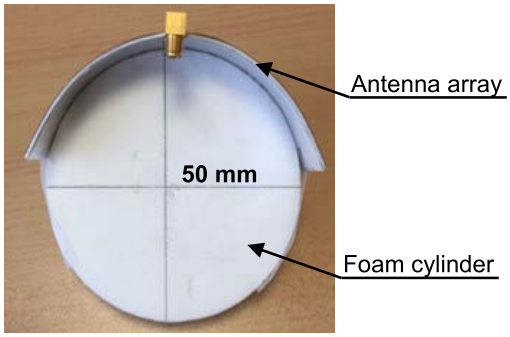

FIGURE 14. Fabricated FPMC antenna array bent on a 50 mm-radius foam cylinder.

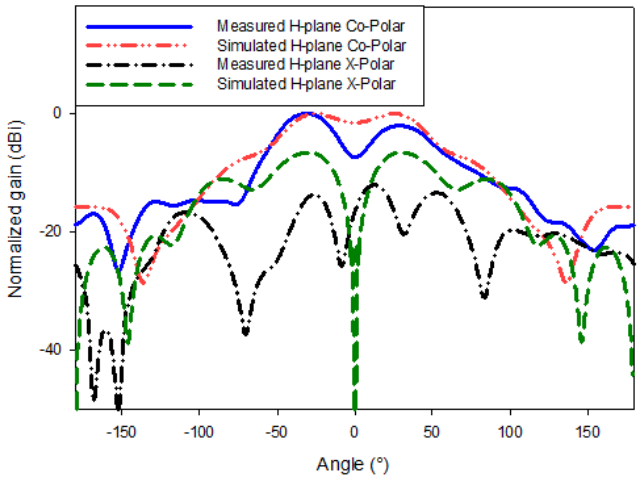

FIGURE 15. Simulated and measured radiation patterns at 5.8 GHz of the FPMC antenna array bent on a 50 mm-radius foam cylinder.

The worst case of the bending configuration (50 mm-radius) has been considered experimentally. Therefore, the fabricated antenna array was bent on a cylinder made of Rohacell foam (the same foam used to fabricate the FPMC antenna array, Fig. 14), and the related radiation patterns were measured, and compared with those of the numerical results (Fig. 15).

The deformation of the measured radiation patterns is also clearly noticed. This phenomenon is explained by the weak contribution of the two extreme patches at the end of the array. In planar configuration, each patch is in-phase when the radiation beam points in the axis. In the bending configuration, each patch of the antenna array presents a phase shift following the bending radius. The impact of the phase shift becomes more important as the patches are located at the edges of the array (Fig. 16).

To circumvent this behavior, it is necessary to offset the phase shift by adding phase shifters to the microstrip feeding lines of the two peripheral patches. In microstrip technology, any additional line in excess of a reference introduces a phase shift. The actual length of the required transmission

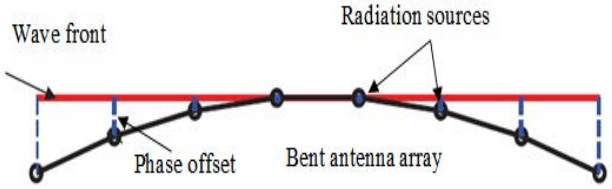

FIGURE 16. Bent N-patches antenna array with isotropic sources pointing in the axis.

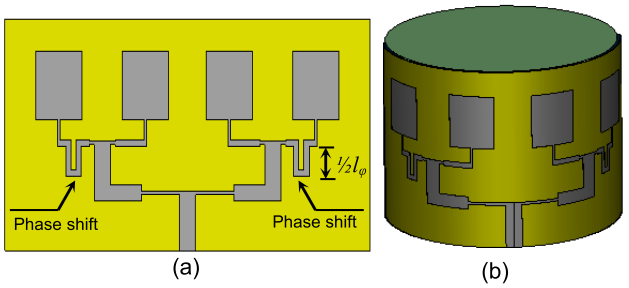

FIGURE 17. Simulated FPMC antenna array with 100°-phase shifters at both endpoints patch antennas. (a) layout. (b) curved on a 50 mm-radius air cylinder.

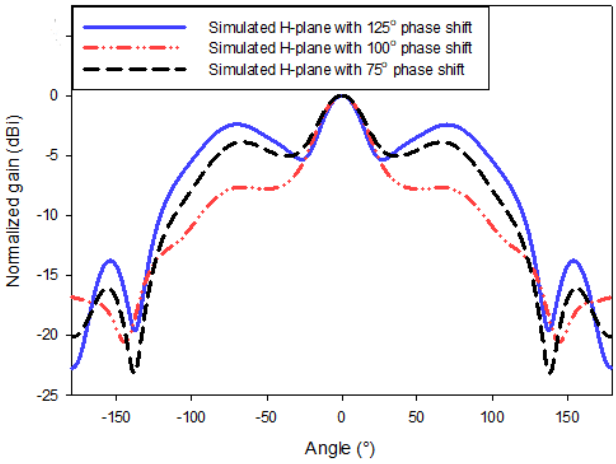

FIGURE 18. Simulated radiation patterns at 5.8 GHz of the FPMC antenna array after bending on a 50 mm-radius air cylinder with 125°, 100°, and 75°-phase shifters.

line is obtained from (3) and (4) according to [43], as follows:

$$l_\varphi = \frac{\lambda_g}{360} \times \Delta\varphi \tag{3}$$

$$\lambda_g = \frac{c}{f_r} \times \frac{1}{\sqrt{\varepsilon_{eff}}} \tag{4}$$

where l_φ is the actual required length to offset for phase shift, $\Delta\varphi$ is the phase shift angle (in degrees), and λ_g is the guided wavelength at the operating frequency. The FPMC antenna array has been simulated after adding the phase shifters (Fig. 17(a)) and then bending on a 50 mm-radius air cylinder (Fig. 17(b)). l_φ has been adjusted to obtain different phase

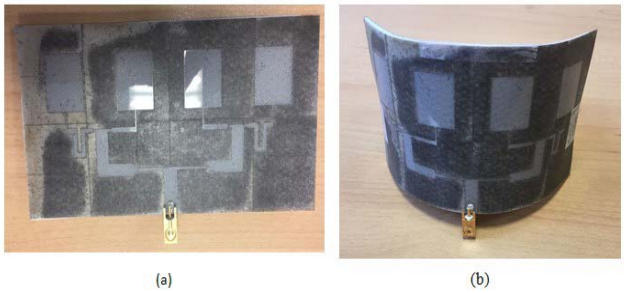

FIGURE 19. Photographs of the fabricated FPMC antenna array with 100°-phase shifters at both endpoints patch antennas. (a) in a flat configuration. (b) in bending configuration on a 50 mm-radius foam cylinder.

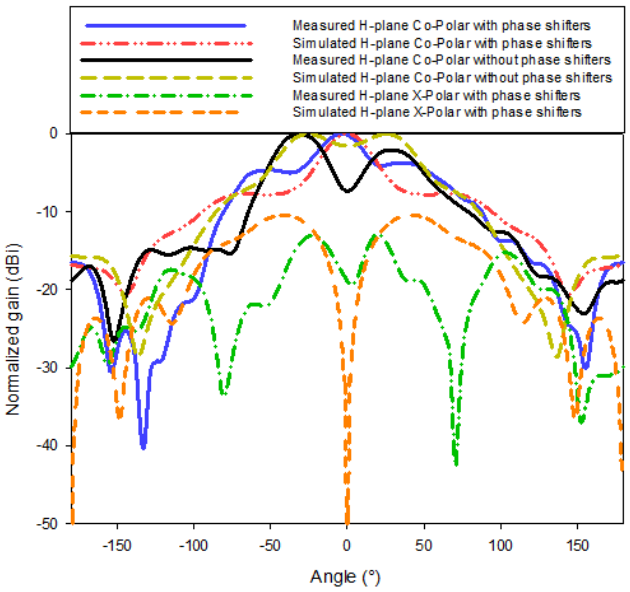

FIGURE 20. Simulated and measured radiation patterns at 5.8 GHz of the FPMC antenna array with and without 100°-phase shifters and bent on a 50 mm-radius foam cylinder.

shifts (125°, 100°, and 75°) and to achieve the suitable phase offset angle. As depicted in Fig. 18, the 100°-phase shift provides the relevant radiation pattern correction. Accordingly, a new FPMC antenna array has been fabricated by adding 100°-phase shifters at both endpoints patch antennas.

The fabricated FPMC antenna array with 100°-phase shifters is then bent on a 50 mm-radius Rohacell foam cylinder (Fig. 19(b)) and characterized at 5.8 GHz.

The measured results are in good agreement with the simulated ones (Fig. 20). The radiation pattern deformation is strongly reduced, and thereby a significant decrease of the SLL and a significant enhancement of the main lob level are noticed. Indeed, the SLL is close to −13 dB for the simulated flat antenna array configuration and close to −8 dB for the simulated bent one with 100°-phase shifters, compared with −5 dB for the measured bent configuration. Moreover, the difference in the gain level between the flat and the bent

configurations (11.9 dBi against 8.7 dBi respectively, Table 3) may also be due to a fringing E-field effect by the edge of the patches. In the flat configuration, a part of the radiation would be added up in phase along the radiation direction. In contrast of the bent configuration, the fringing E–fields at some parts of the bent FPMC antenna array would be no longer added up in the same phase of the radiation direction. As a result, this phenomenon causes a deterioration in the gain level and a variation in the radiation patterns compared with those of the flat configuration.

Furthermore, the FPMC antenna array exhibits high measured efficiency, especially at the central operating frequency (5.8 GHz) for which the antenna array is well matched: 75% against 71% without any phase shifter (Table 3).

TABLE 3. Simulated and measured gains and efficiencies of the FPMC antenna arrays in flat and bending configurations on a 50 mm-radius with and without 100°-phase shifters.

	Flat antenna array without phase shifters	Bent antenna array without phase shifters	Bent antenna array with phase shifters
Simulated gain (dBi)	12.9	6.1	8.6
Measured gain (dBi)	11.9	6.6	8.7
Simulated efficiency (%)	76	70	72
Measured efficiency (%)	75	71	75

VI. CONCLUSION

An innovative route has been proposed and investigated to fabricate FPMC antenna arrays for conformal applications. The FPMC antenna arrays were fabricated using a conductive mesh-style fabric stacked on E-glass-fiber mat tissue and infused with epoxy resin. Such composite antenna arrays present high mechanical flexibility under bending, low ohmic loss by using a 57 μm-thick highly conductive fabric, and low dielectric loss by inserting a 1 mm-thick foam layer between the radiating elements and the ground plane. The 50 mm-radius bending effects on the radiation pattern of the antenna array were minimized by adding 100°-phase shifters at the feeding lines of both endpoints patch antennas. The high radiation performance in gain and efficiency at 5.8 GHz (11.9 dBi and 75% in a flat configuration; 8.7 dBi and 75% in 50 mm-radius bending configuration), the seamless integration process, and the flexible mechanical properties of such composite antenna arrays pave the way for their promising and efficient integration into various devices, objects and vehicles made of composite laminate materials for the wireless and 5G networks.

REFERENCES

[1] K. K. Kar, *Composite Materials: Processing, Applications, Characterizations*. Berlin, Germany: Springer, 2017, Accessed: May 26, 2020. [Online]. Available: https://www.academia.edu/36174277/Composite_Materials_Processing_Applications_Characterizations

[2] S. Kangishwar, N. Radhika, A. A. Sheik, A. Chavali, and S. Hariharan, "A comprehensive review on polymer matrix composites: Material selection, fabrication, and application," *Polym. Bull.*, vol. 79, no. 2, pp. 1–41, Jan. 2022.

[3] D. Pathania and D. Singh, "A review on electrical properties of fiber reinforced polymer composites," *Int. J. Theor. Appl. Sci.*, vol. 1, no. 2, pp. 34–37, 2009.

[4] J. Hinrichsen, "Airbus A380: Requirements for the selection of materials and manufacturing technologies," *ATB Métallurgie*, vol. 41, no. 3, pp. 24–30, 2001.

[5] P. N. Vines, A. G. Garcia, and C. C. Pancorbo, "Method for manufacturing elements of composite materials by the co-bonding technique," U.S. Patent 6 735 866, May 18, 2004.

[6] B. D. Pell, E. Sulic, W. S. T. Rowe, K. Ghorbani, and S. John, *Advancements in Automotive Antennas: New Trends and Developments in Automotive System Engineering*. Rijeka, Croatia: Intech Open Science, 2011. [Online]. Available: http://www.intechopen.com/books/new-trends-and-developments-in-automotive-system-engineering/advancements-in-automotive-antennas

[7] S. Rana and R. Fangueiro, *Advanced Composite Materials for Aerospace Engineering: Processing, Properties and Applications*. Duxford, U.K.: Elsevier, Apr. 2016. [Online]. Available: https://www.elsevier.com/books/advanced-composite-materials-for-aerospace-engineering/rana/978-0-08-100037-3

[8] F. M. Al-Oqla and S. M. Sapuan, "Natural fiber reinforced polymer composites in industrial applications: Feasibility of date palm fibers for sustainable automotive industry," *J. Cleaner Prod.*, vol. 66, pp. 347–354, Mar. 2014.

[9] E. Mangino, J. Carruthers, and G. Pitarresi, "The future use of structural composite materials in the automotive industry," *Int. J. Veh. Des.*, vol. 44, nos. 3–4, pp. 211–232, Jan. 2007.

[10] S. Sajan and D. P. Selvaraj, "A review on polymer matrix composite materials and their applications," *Mater. Today, Proc.*, vol. 47, pp. 5493–5498, Sep. 2021.

[11] M. Won, T. Park, and S. H. Son, "Toward mitigating phantom jam using vehicle-to-vehicle communication," *IEEE Trans. Intell. Transp. Syst.*, vol. 18, no. 5, pp. 1313–1324, May 2017.

[12] O. V. Mukbaniani, D. Balköse, H. Susanto, and A. Haghi, *Composite Materials for Industry, Electronics, and the Environment: Research and Applications*. Palm Bay, FL, USA: CRC Press, Jun. 3, 2019. [Online]. Available: https://www.taylorfrancis.com/books/edit/10.1201/9780429457937/composite-materials-industry-electronics-environment-omari-mukbaniani-devrim-balk%C3%B6se-heru-susanto-haghi

[13] M. A. Leeds, *Electronic Properties of Composite Materials, Handbook of Electronics Materials*. New York, NY, USA: Springer, Mar. 2013, doi: 10.1007/978-1-4615-9612-7.

[14] L. Manac'h, X. Castel, and M. Himdi, "Performance of a lozenge monopole antenna made of pure composite laminate," *Prog. Electromagn. Res. Lett.*, vol. 35, pp. 115–123, 2012.

[15] M. Lila, F. Kumar, and S. Sharma, "Composites from waste for civil engineering applications," *I-Manager's J. Mater. Sci.*, vol. 1, no. 3, pp. 1–11, Dec. 2013.

[16] H. Rmili, J. L. Miane, H. Zangar, and T. Olinga, "Design of microstrip-fed proximity-coupled conducting-polymer patch antenna," *Microw. Opt. Technol. Lett.*, vol. 48, no. 4, pp. 655–660, Apr. 2006.

[17] Y. Bayram, Y. Zhou, B. S. Shim, S. Xu, J. Zhu, N. A. Kotov, and J. L. Volakis, "E-textile conductors and polymer composites for conformal lightweight antennas," *IEEE Trans. Antennas Propag.*, vol. 58, no. 8, pp. 2732–2736, May 2010.

[18] A. Ameli, P. U. Jung, and C. B. Park, "Electrical properties and electromagnetic interference shielding effectiveness of polypropylene/carbon fiber composite foams," *Carbon*, vol. 60, pp. 379–391, Aug. 2013.

[19] R. Tellakula, V. Varadan, T. Shami, and G. Mathur, "Carbon fiber and nanotube based composites with polypyrrole fabric as electromagnetic absorbers," *Smart Mater. Struct.*, vol. 13, no. 5, p. 1040, Jul. 2004.

[20] I. M. De Rosa, F. Sarasini, M. S. Sarto, and A. Tamburrano, "EMC impact of advanced carbon fiber/carbon nanotube reinforced composites for next-generation aerospace applications," *IEEE Trans. Electromagn. Compat.*, vol. 50, no. 3, pp. 556–563, Aug. 2008.

[21] C. L. Holloway, M. S. Sarto, and M. Johansson, "Analyzing carbon-fiber composite materials with equivalent-layer models," *IEEE Trans. Electromagn. Compat.*, vol. 47, no. 4, pp. 833–844, Nov. 2005.

[22] W. Bauhofer and J. Z. Kovacs, "A review and analysis of electrical percolation in carbon nanotube polymer composites," *Compos. Sci. Technol.*, vol. 69, no. 10, pp. 1486–1498, Aug. 2009.

[23] R. K. Challa, D. Kajfez, V. Demir, J. R. Gladden, and A. Z. Elsherbeni, "Characterization of multiwalled carbon nanotube (MWCNT) composites in a waveguide of square cross section," *IEEE Microw. Wireless Compon. Lett.*, vol. 18, no. 3, pp. 161–163, Mar. 2008.
[24] A. Mehdipour, C. W. Trueman, A. R. Sebak, and S. V. Hoa, "Carbon-fiber composite T-match folded bow-tie antenna for RFID applications," in *Proc. IEEE Antennas Propag. Soc. Int. Symp.*, North Charleston, SC, USA, Jun. 2009, pp. 1–4.
[25] C. Buccella, "Quasi-stationary analysis of the electric field in anisotropic laminated composites," *IEEE Trans. Ind. Appl.*, vol. 35, no. 6, pp. 1296–1305, Nov. 1999.
[26] Y. Huang, N. Li, Y. Ma, F. Du, F. Li, X. He, X. Lin, H. Gao, and Y. Chen, "The influence of single-walled carbon nanotube structure on the electromagnetic interference shielding efficiency of its epoxy composites," *Carbon*, vol. 45, no. 8, pp. 1614–1621, Jul. 2007.
[27] A. Mehdipour, A.-R. Sebak, C. W. Trueman, I. D. Rosca, and S. V. Hoa, "Performance of microstrip patch antenna on a reinforced carbon fiber composite ground plane," *Microw. Opt. Technol. Lett.*, vol. 53, pp. 1328–1331, Jun. 2011.
[28] A. Mehdipour, A.-R. Sebak, C. W. Trueman, I. D. Rosca, and S. V. Hoa, "Reinforced continuous carbon-fiber composites using multi-wall carbon nanotubes for wideband antenna applications," *IEEE Trans. Antennas Propag.*, vol. 58, no. 7, pp. 2451–2456, Jul. 2010.
[29] T. Matsunaga, K. Matsuda, T. Hatayama, K. Shinozaki, and M. Yoshida, "Fabrication of continuous carbon fiber-reinforced aluminum–magnesium alloy composite wires using ultrasonic infiltration method," *Compos. A, Appl. Sci. Manuf.*, vol. 38, no. 8, pp. 1902–1911, Aug. 2007.
[30] L. Manac'h, X. Castel, and M. Himdi, "Microwave performance of a carbon composite antenna," in *Proc. Eur. Microw. Conf.*, Nuremberg, Germany, Oct. 2013, pp. 770–773.
[31] H. A. E. Elobaid, S. K. A. Rahim, M. Himdi, X. Castel, and M. A. Kasgari, "A transparent and flexible polymer-fabric tissue UWB antenna for future wireless networks," *IEEE Antennas Wireless Propag. Lett.*, vol. 16, pp. 1333–1336, 2016.
[32] A. Mehdipour, I. D. Rosca, A. Sebak, C. Trueman, and S. Hoa, "Advanced carbon-fiber composite materials for RFID tag antenna applications," *Appl. Comput. Electromagn. Soc. J.*, vol. 25, no. 3, pp. 218–229, Mar. 2010.
[33] A. Mehdipour, I. D. Rosca, A.-R. Sebak, C. W. Trueman, and S. V. Hoa, "Full-composite fractal antenna using carbon nanotubes for multiband wireless applications," *IEEE Antennas Wireless Propag. Lett.*, vol. 9, pp. 891–894, 2010.
[34] P. B. Samal, P. J. Soh, and G. A. E. Vandenbosch, "UWB all-textile antenna with full ground plane for off-body WBAN communications," *IEEE Trans. Antennas Propag.*, vol. 62, no. 1, pp. 102–108, Jan. 2014.
[35] M. Klemm and G. Troester, "Textile UWB antennas for wireless body area networks," *IEEE Trans. Antennas Propag.*, vol. 54, no. 11, pp. 3192–3197, Nov. 2006.
[36] C.-P. Lin, C.-H. Chang, Y. T. Cheng, and C. F. Jou, "Development of a flexible SU-8/PDMS-based antenna," *IEEE Antennas Wireless Propag. Lett.*, vol. 10, pp. 1108–1111, 2011.
[37] C. A. Balanis, *Antenna Theory: Analysis and Design*, 4th ed. Hoboken, NJ, USA: Wiley, 2016.
[38] S. Sevak, "Design and evaluation of high gain microstrip patch antenna using double layer with air gap," *Int. J. Recent Innov. Trends Comput. Commun.*, vol. 3, no. 3, pp. 1678–1681, 2015.
[39] S. Bedra and R. Bedra, "Radiation characteristics of circular microstrip patch antenna with and without air-gap using neuro-spectral computation approach," *WSEAS Trans. Commun.*, vol. 13, pp. 340–347, Jan. 2014.
[40] M. Gupta, S. Sachdeva, N. K. Swamy, and I. P. Singh, "Rectangular microstrip patch antenna using air as substrate for S-band communication," *J. Electromagn. Anal. Appl.*, vol. 6, no. 3, pp. 38–41, 2014.
[41] M. Jamlos, T. Rahman, M. Kamarudin, M. Ali, M. M. Tan, and P. Saad, "The gain effects of air gap quadratic aperture-coupled microstrip antenna array," in *Proc. PIERS*, Cambridge, MA, USA, Jul. 2010, pp. 462–465.
[42] S. Bedra, R. Bedra, S. Benkouda, and T. Fortaki, "Full-wave analysis of anisotropic circular microstrip antenna with air gap layer," *Prog. Electromagn. Res. M*, vol. 34, pp. 143–151, 2014.
[43] S. AliyuBabale, S. H. Lawan, S. K. A. Rahim, and S. IfeomaOrakwue, "Implimentation of 4×4 Butler matrix using silver-nono instant inkjet printing technology," in *Proc. IEEE 3rd Int. Conf. Electro-Technol. Nat. Develop. (NIGERCON)*, Owerri, Nigeria, Nov. 2017, pp. 514–518.

HUSAMELDIN ABDELRAHMAN ELMOBARAK received the Ph.D. degree in wireless communications from the Wireless Communication Centre (WCC), Faculty of Electrical Engineering, Universiti Teknologi Malaysia (UTM), Johor, Malaysia, in 2018. He worked as a Researcher at the Institut d'Electronique et des Technologies du numéRique (IETR UMR-CNRS 6164), University of Rennes 1, France, from 2020 to 2021. He is currently an Assistant Professor at the Department of Electrical and Electronics Engineering, Faculty of Engineering Science, OIU University, Sudan. His research interests include flexible and conformal antenna applications, flexible materials for flexible antennas, wearable antennas, nano-materials, and 2D materials for antenna applications and smart antennas. He was a recipient of three scientific awards.

MOHAMED HIMDI received the Ph.D. degree in signal processing and telecommunications from the University of Rennes 1, France, in 1990. Since 2003, he has been a Professor with the University of Rennes 1 and the Head of the High Frequency and Antenna Department, IETR, since 2013. He has authored or coauthored 151 journal articles and over 350 papers in conference proceedings. He has also coauthored ten book chapters. He holds 46 patents. His research interests include passive and active millimeter-wave antennas, development of new architectures of antenna arrays, and new three-dimensional (3D) antenna technologies. He was a Laureate of the 2D National Competition for the Creation of Enterprises in Innovative Technologies (Ministry of Industry and Education), in 2000. In March 2015, he received the JEC-AWARD at Paris on pure composite material antenna embedded into a motorhome roof for the digital terrestrial television reception. He also received the Valorization Trophy 2021 from the Rennes Innovation Campus.

XAVIER CASTEL received the Ph.D. degree in material science from the University of Rennes 1, Rennes, France, in 1997. From 1999 to 2016, he was an Associate Professor with the Technological Institute of Saint-Brieuc, University of Rennes 1, Saint-Brieuc, France, and a Researcher with the Institut d'Electronique et des Technologies du numéRique (IETR UMR-CNRS 6164), University of Rennes 1, where he was nominated as a Full Professor, in 2017. He is currently the Co-Head of the Functional Materials Team and of the Antennas and Microwave Devices Department. He has authored and coauthored about 60 international papers, more than 245 conference presentations, and holds 22 patents. His main research interests include the elaboration of advanced materials (transparent and conducting materials, superconductors, semiconductors, and composite materials) for microwave applications, their physical-chemical characterizations (electrical, optical, structural, microstructural, thermal, and mechanical properties), and the fabrication of the related microwave devices and antennas (by photolithographic technique, wet-etching process, lift-off process, laser micro-etching; contact molding, vacuum infusion, compression molding, and prepreg processes). He was a recipient and a co-recipient of eight scientific awards.

SHARUL KAMAL ABDUL RAHIM received the degree in electrical engineering from The University of Tennessee, Knoxville, TN, USA, the M.Sc. degree in engineering (communication engineering) from Universiti Teknologi Malaysia (UTM), and the Ph.D. degree in wireless communication system from the University of Birmingham, U.K., in 2007. After he graduated from The University of Tennessee, he spent three years in the industry. After graduated from the M.Sc. degree, he joined UTM, in 2001, where he is currently a Professor at the Wireless Communication Centre. He has published over 200 learned articles in journals, including *IEEE Antenna and Propagation Magazine*, the IEEE TRANSACTIONS ON ANTENNA AND PROPAGATION, and the IEEE ANTENNA AND PROPAGATION LETTERS. He also has many patents. His research interests include antenna design, smart antenna systems, beamforming networks, and microwave devices for fifth generation mobile communication. He is a Senior Member of the IEEE Malaysia Section, a member of the Institute of Engineer Malaysia, a Professional Engineer with BEM, a member of the Eta Kappa Nu Chapter, University of Tennessee, and the International Electrical Engineering Honor Society. He is currently an Executive Committee Member of the IEM Southern Branch.

TAN KIM GEOK received the B.E., M.E., and Ph.D. degrees all in electrical engineering from the University of Technology Malaysia, in 1995, 1997, and 2000, respectively. He has been a Senior Research and Development Engineer at EPCOS Singapore, since 2000. From 2001 to 2003, he joined DoCoMo Euro-Laboratories, Munich, Germany. He is currently an Academic Staff at Multimedia University. His research interests include radio propagation for outdoor and indoors, RFID, multi-user detection technique for multi-carrier technologies, and A-GPS.